International Journal of Ocean Engineering and Technology Vol. 3, No. 1, pp 8~13, April 2000 (ISSN 1229-1668)

Theoretical Investigation on the Singularity System to Represent Two Circular Cylinders in an Inviscid Flow*

D. K. Lee

School of Transportation Systems Engineering, University of Ulsan 680-749, Korea

(Received 11 January 2000, accepted 29 February 2000)

KEY WORDS. image singularity system, two circular cylinders, discrete vortex method, vortex shedding

ABSTRACT *The singularity system to represent two circular cylinders poised under different ambient flow fields is considered in the present research. The singularity system, being composed of a series of singularities, has to be truncated for numerical calculations. A rational criterion to determine how many terms of this series should be retained to maintain the prescribed accuracy is provided through analysis of the converging property of the series.*

A particular emphasis is put to how to deal with the discrete vortex model of a boundary layer, this possibility being the basis for the development of a tool to simulate vortex shedding from a structure composed of two circular cylinders.

The principle to obtain the present singularity system can be applied to more-than-two-cylinders structure. Only the series become much more complex with increase of the number of cylinders.

1. Introduction

When a single circular cylinder is present in the two-dimensional irrotational flow field the complex potential is defined and the singularity system representing the cylinder can be readily found. The Milne-Thomson's circle theorem(1) proves to be an efficient tool in this process if used with some care

However, when there are more than one circular cylinders in the flow field, the singularity system to represent each cylinder cannot be obtained at a glance due to the interactions between the cylinders. The circle theorem can still be applied for one cylinder at a particular stage but the result accompanies violation of the boundary condition on the other cylinder. This fact makes it more convenient to compose the singularity system with the concept of image singularity than with help of the circle theorem.

Only the case of two circular cylinders has been considered in the present study because this is the basic case in that the principle improvised herein can be applied without alteration to other cases with even more circular cylinders. However, the complexity of the singularity system grows extremely rapidly with increase of the number of the cylinders.

The knowledge of the potential flow in the two-dimensional flow field with multiple circular cylinders is necessary in connection with several contexts. The potential flow itself can be of some value in its own sake or as the basis for further theoretical and/or numerical analysis. Another good examples may be found in the simulation of vortex shedding from multiple cylinders by discrete vortex method. The possibility of this latter application has in fact been the motivation of the present study.

2. The basic complex potentials

Let us cite here for the later use some well known complex potentials(2) describing a few basic flow fields:

uniform stream ; $\varphi(z)=\underline{W}e^{-i\alpha}z$ (2.1)

vortex located at ζ ; $\varphi(z)=-\frac{i\Gamma}{2\pi}\log(z-\zeta)$ (2.2)

dipole located at ξ ; $\varphi(z)=-\mu\frac{e^{i\beta}}{z-\xi}$ (2.3)

Now, suppose that we introduce a cylinder of radius a in each of these flow fields. Application of the circle theorem gives us the following results.

1) Basic case I ; a cylinder in uniform stream

* the complex potential

$$\varphi(z)=\underline{W}e^{-i\alpha}z-\underline{W}a^2\frac{e^{i(\pi+\alpha)}}{z} \quad (2.4)$$

* the image system ; one dipole

strength ; $\mu=\underline{W}a^2$

location ; the center of the cylinder

axis ; $\beta=\pi+\alpha$

2) Basic case II ; a cylinder with its center at z_c in the flow field created by a vortex of the strength Γ

* the complex potential

* This work was supported by UOU reseasch promotion fund in 1997

$$\varphi(z) = -\frac{i\Gamma}{2\pi}[\log(z-\zeta) - \log(z-\zeta i) + \log(z-\zeta_c)] \quad (2.5)$$

* the image system ; two vortices

strengths ; $\Gamma_i = -\Gamma, \quad \Gamma_c = \Gamma$

locations ; $\zeta_i = a^2/\bar{\zeta}, \quad \zeta_c = z_c$

3) Basic case III ; a cylinder with its center at the origin in the flow field created by a dipole of the strength μ and the axis rotated an angle β from the x-coordinate

* the complex potential

$$\varphi(z) = -\mu\frac{e^{i\beta}}{z-\xi} - \mu_i\frac{e^{i\beta_i}}{z-\xi_i} \quad (2.6)$$

with $\xi = \sigma e^{i\theta}$

* the image system ; one dipole

strength ; $\mu_i = \mu\,(a/\sigma)^2$

location ; $\xi_i = a^2/\bar{\xi}$;

axis ; $\beta_i = \pi + 2\theta - \beta$

4) Basic case IV ; a cylinder located at the origin with a vortex shed from it

* the complex potential

$$\varphi(z) = -\frac{i\Gamma}{2\pi}[\log(z-\zeta) - \log(z-\zeta_i)] \quad (2.7)$$

* the image system ; one vortex

strength ; $\Gamma_i = -\Gamma$

location ; $\zeta_i = a^2/\bar{\zeta}$,

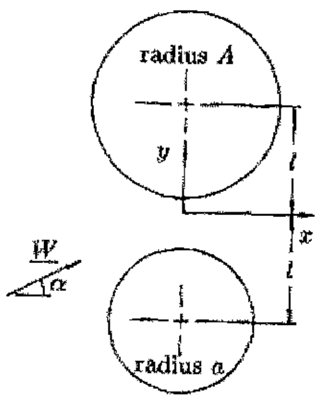

Figure. 1 Uniform flow

3. Two cylinders in a uniform flow

Let us consider the potential flow around two circular cylinders of different radii arranged as shown in Figure 1 and try to satisfy the boundary condition on the surface of the both cylinders. The process may be best explained in a step by step fashion as follows.

(1) the initial step

Each cylinder is represented by a dipole as described in the basic case I as if it exists alone in the uniform flow field. Thus we have:

* for the cylinder 1

strength ; $\mu_{10} = \underline{W}A^2$

position ; $\xi_{10} = il$

axis ; $\beta_{10} = \pi + \alpha$

* for the cylinder 2

strength ; $\mu_{20} = \underline{W}a^2$

position ; $\xi_{20} = -il$

axis ; $\beta_{20} = \pi + \alpha$

(2) the first step

The dipoles introduced in the initial step changes the nature of the external flow with respect to each cylinder, bringing the necessity of the image dipole according to the concept of the basic case III.

* for the cylinder 1

strength ; $\mu_{11} = \mu_{20}\, A^2/\,(l + |\xi_{20}|)^2$

position ; $\xi_{11} = A^2/(\bar{\xi}_{20} + il) + il$

axis ; $\zeta_{11} = \pi - \alpha$

* for the cylinder 2

strength ; $\mu_{21} = \mu_{10}\, a^2/\,(l + |\xi_{10}|)^2$

position ; $\xi_{21} = a^2/(\bar{\xi}_{10} - il) - il$

axis ; $\beta_{21} = \pi - \alpha$

(3) the second step

The dipoles of the above step further modifies the external flow with regard to each cylinder. The boundary condition demands the image dipole within each cylinder to match the dipole newly introduced in the first step within the other cylinder. The characteristics of the required dipoles are:

* for the cylinder 1

strength ; $\mu_{12} = \mu_{21}\, A^2/\,(l + |\xi_{21}|)^2$

position ; $\xi_2 = A^2/(\bar{\xi}_{21} + il) + il$

axis ; $\beta_{12} = \pi + \alpha$

* for the cylinder 2

strength ; $\mu_{22} = \mu_{11}\, a^2/\,(l + |\xi_{11}|)^2$

position ; $\xi_{22} = a^2/(\bar{\xi}_{11} - il) - il$

axis ; $\beta_{22} = \pi + \alpha$

(4) the third step

This process continues indefinitely. Thus the image singularity system is composed of a series of infinite number of dipoles lined up on a segment of the imaginary axis within each circle. It is to be noted that the dipole strength diminishes as the above step of process advances.

The complex potential describing the flow field is then expressed, after nondimensionalized with respect to the free stream speed W and the radius A of the major cylinder, as follows.

$$\varphi(z)= e^{-i\alpha}z+ \varphi_d(z) \tag{3.1}$$

where $\varphi_d(z)$ denotes the complex potential due to the series of dipoles and is expressed as:

$$\varphi_d(z)= \mu_{10}\frac{e^{i\alpha}}{z-\xi_{10}}+\mu_{11}\frac{e^{-i\alpha}}{z-\xi_{11}}+\cdots \tag{3.2}$$

$$+\mu_{20}\frac{e^{i\alpha}}{z-\xi_{20}}+\mu_{21}\frac{e^{-i\alpha}}{z-\xi_{21}}+\cdots$$

where $\mu_{1k}=\mu_{2(k-1)}\dfrac{1}{(|\xi_{2(k-1)}-is/2|)^2}$

$$\mu_{2k}=\mu_{1(k-1)}\frac{r^2}{(|\xi_{1(k-1)}+is/2|)^2}$$

$$\xi_{1k}=\frac{1}{\bar{\xi}_{2(k-1)}+is/2}+i\frac{s}{2}$$

$$\xi_{2k}=\frac{r^2}{\bar{\xi}_{1(k-1)}-is/2}-i\frac{s}{2}$$

$$\mu_{10}=1,\quad \mu_{20}=r^2$$

$$\xi_{10}=is/2,\quad \xi_{20}=-is/2$$

$$s=2l/A,\ r=a/A$$

4. Uniform flow with the shed vortices

Suppose that the vortex shedding is simulated by discrete vortices within the approximation of the potential flow modelling. To start with, consider a particular single vortex shed from one of the cylinders as shown in Figure 2. Following the principle of the basic case IV, an image vortex appears at the inverse point within the cylinder. Now, these two vortices have to be respectively met by the two image vortices within the other cylinder. Then these latter two vortices call for still further two image vortices within the first cylinder. This process continues indefinitely and may be explained again in a step by step fashion.

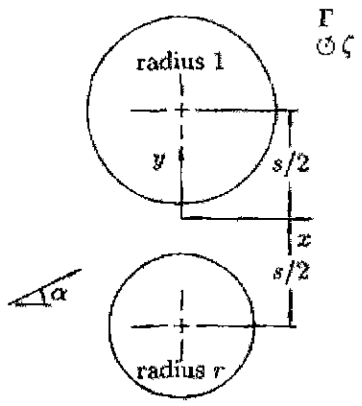

Figure. 2 Uniform flow with a vortex

The total complex potential would be given by the superposition of the complex potential representing the uniform flow about the cylinders and that due to these series of the vortices.

$$\varphi(z)= e^{-i\alpha}z+ \varphi_d(z)+ \varphi_v(z) \tag{4.1}$$

$\varphi_v(z)$ coming from the series of the vortices takes the following form when nondimensionalized.

$$\varphi_v(z)=-\frac{i\Gamma}{2\pi}\log(z-\zeta) \tag{4.2}$$

$$+\frac{i\Gamma}{2\pi}[\log(z-\zeta_{11})-\log(z-\zeta_{12})+\cdots]$$

$$+\frac{i\Gamma}{2\pi}[\log(z-\zeta_{21})-\log(z-\zeta_{22})+\cdots]$$

where $\zeta_{1k}=c_{1k}+is/2,\ \zeta_{2k}=c_{2k}-is/2$ (4.3)

ζ_{1k} and ζ_{2k} denote the position of the image vortices within the cylinder 1 and the cylinder 2 respectively, and c_{1k} and c_{2k} represent the complex position vectors of each of these image vortices relative to the center of the respective cylinder it belongs to and are given by;

$$c_{1k}=\frac{1}{\bar{\zeta}_{2(k-1)}+is/2},\quad c_{2k}=\frac{r^2}{\bar{\zeta}_{1(k-1)}-is/2} \tag{4.4}$$

with $\zeta_{10}=\zeta_{20}=\zeta$

When there are N_1 and N_2 vortices in the flow field shed respectively from the cylinder 1 and the cylinder 2, the complex potential would be given as

$$\varphi(z)= e^{-i\alpha}z+\varphi_d(z)$$

$$+\sum_{j=1}^{2}\sum_{k=1}^{N_j}\varphi_v(z,\ (\Gamma)_{jk},\ (\zeta)_{jk}) \tag{4.5}$$

in which $\varphi_v(z,\ (\Gamma)_{jk},\ (\zeta)_{jk})$ is just $\varphi_v(z)$ of eq.(4.2) with Γ and ζ replaced respectively by $(\Gamma)_{jk}$ and $(\zeta)_{jk}$.

5. Truncation of the infinite series

5.1 Truncation of the series for φ_d

For this purpose, it would be sufficient to consider the series of μ's rather than φ_d itself and, moreover, only the series of μ's within either series. Let this series be denoted by S_μ, that is,

$$S_\mu=\mu_0+\mu_1+\cdots+\mu_{m-1}+R_{\mu m} \tag{5.1}$$

$$\text{where}\quad R_{\mu m}=\mu_m+\mu_{m+1}+\cdots \tag{5.2}$$

It can be recognized without difficulty that this series most slowly converges when the two cylinders have the same radius, i.e. when $r=1$. If so, μ's are expressed as:

$$\mu_k=\prod_{j=1}^{k}g_j^2\quad \text{for } k=1,2,\cdots\quad \text{with}\quad \mu_0=1 \tag{5.3}$$

where $g_1 = \frac{h_1}{s-}\frac{h_2}{s-}\cdots\frac{h_{j-1}}{s-}\frac{h_j}{s}$ (5.4)

and $h_1 = h_2 = \cdots = h_j = 1$

If the cylinders are not in contact, s is greater than 2 and hence

$$g_k < g_{k+1} < \frac{1}{s-1} \quad \text{for } k=1,2,\cdots \qquad (5.5)$$

From these inequalities, we can deduce that

$$R_{\mu m} < \frac{1}{[(s-1)^2-1](S-1)^{2(m-1)}} \qquad (5.6)$$

Equating the right hand side of this expression to a certain prespecified small number ε_μ, we can fix the number of terms M_d to be retained to keep the sum of the neglected terms within the desired error bound.

$$M_d - 1 < 1 - \frac{\log[\varepsilon_\mu s(s-2)]}{2\log(s-1)} \leq M_d \qquad (5.7)$$

5.2 Truncation of the series for φ_v

Consider the series for $\varphi_v(z)$ excluding the external vortex term and the two leading image vortex terms. The remaining series can be expanded as the following;

$$\begin{aligned}\varphi_v'(z) = &-\frac{i\Gamma}{2\pi}\left\{\left[\frac{\Delta\zeta_{12}}{z-\zeta_{12}} + \frac{(\Delta\zeta_{12})^2}{2(z-\zeta_{12})^2} + \cdots\right]\right.\\ &\left.+\left[\frac{\Delta\zeta_{14}}{z-\zeta_{14}} + \frac{(\Delta\zeta_{14})^2}{2(z-\zeta_{14})^2} + \cdots\right] + \cdots\right\}\\ &-\frac{i\Gamma}{2\pi}\left\{\left[\frac{\Delta\zeta_{22}}{z-\zeta_{22}} + \frac{(\Delta\zeta_{22})^2}{2(z-\zeta_{22})^2} + \cdots\right]\right.\\ &\left.+\left[\frac{\Delta\zeta_{24}}{z-\zeta_{24}} + \frac{(\Delta\zeta_{24})^2}{2(z-\zeta_{24})^2} + \cdots\right] + \cdots\right\}\end{aligned} \qquad (5.8)$$

where $\Delta\zeta_{1k} = \zeta_{1(k+1)} - \zeta_{1k}$

$\Delta\zeta_{2k} = \zeta_{2(k+1)} - \zeta_{2k}$ (5.9)

The inverse points ζ_{1k} and ζ_{2k} in eq.(4.2) and the above equations have the following properties

$$\zeta_{1k} \in \Omega_{(k-1)} \quad \text{and} \quad \zeta_{2k} \in \omega_{(k-1)} \qquad (5.10)$$

where Ω_k ; the image region of the region $\omega_{(k-1)}$

ω_k ; the image region of the region $\Omega_{(k-1)}$

Ω_0 ; the inner region of the cylinder 1

ω_0 ; the inner region of the cylinder 2

Since a subregion will be mapped, according to the circle theorem, into a sub-image region, it is not difficult to see that

$$\Omega_k \subset \Omega_{(k-1)}, \quad \omega_k \subset \omega_{(k-1)} \qquad (5.11)$$

and, hence, the absolute values of $\Delta\zeta_{1k}$ and $\Delta\zeta_{2k}$ are smaller than unity.

Now, for determination of the truncation position of the series eq(5.8) it may be sufficient to consider the following series only,

$$S_{1v} = \Delta\zeta_{12} + \cdots + \Delta\zeta_{1(2m)} + R_{1v(2m)} \qquad (5.12)$$

where $R_{1v(2m)} = \sum_{k=1}^{\infty} \Delta\zeta_{1(2m+2k)}$ (5.13)

in view of the fact that the series comprised of the first order terms converges most slowly. We may think of S_{1v} only because, in fact, the same conclusion is obtained from the consideration of the series composed of $\Delta\zeta_{2k}$.

c_{1k} and c_{2k} as defined by eq.(4.4) take a form of continued fraction. Inserting eq.(4.3) into eq.(5.9) and making use of this property we have, after some manipulation,

$$\frac{\Delta\zeta_{1(2k)}}{\Delta\zeta_{12}} = \prod_{j=1}^{2(k-1)}[c_{1(3+j)}\,\bar{c}_{2(2+j)}/r] \qquad (5.14)$$

for $k=2,3,\cdots$

The properties expressed as eq.(5.11) means that

$$|c_{1k}|_{\max} > |c_{1(k+1)}|_{\max}$$

$$\text{and} \quad |c_{2k}|_{\max} > |c_{2(k+1)}|_{\max} \qquad (5.15)$$

$|c_{1k}|$ and $|c_{2k}|$ become greatest either when $\zeta = (s/2-1)i$ or when $\zeta = -(s/2-r)i$ and we have the maximum values for $|c_{12}|$ and $|c_{22}|$

$$|c_{12}|_{\max} = \frac{1}{s-r}, \quad |c_{22}|_{\max} = \frac{r^2}{s-1} \qquad (5.16)$$

The inequalities shown by eq.(5.15) affirm that

$$\left|\frac{R_{1v(2m)}}{\Delta\zeta_{12}}\right| < \sum_{k=m}^{\infty}\left[\frac{r}{(s-r)(s-1)}\right]^{2k} \qquad (5.17)$$

Suppose a certain small number ε_v is specified to the right hand side of the above equation, that is,

$$\left[\frac{r}{(s-r)(s-1)}\right]^{2m}\frac{1}{1-[r/(s-r)(s-1)]^2} = \varepsilon_v \qquad (5.18)$$

The truncation position $2m$ can be determined from this equation as the smallest even number just greater than the value satisfying the equation. In view of the definition of $\Delta\zeta_{1k}$, let us denote $2m$ so obtained plus 1 by M_v. Then M_v is determined as the smallest odd number satisfying the following inequality.

$$\frac{\log\{\varepsilon_v(1-[r/(s-r)(s-1)]^2\}}{\log[r/(s-r)(s-1)]} + 1 \leq M_v \qquad (5.19)$$

6. The truncated complex potential

The exposition of the previous section makes the truncated version of eq.(4.1) take the following form;

$$\varphi(z) = e^{-i\alpha}z + \sum_{j=1}^{2}\sum_{k=0}^{M_d}\mu_{jk}\frac{1}{z-\xi_{jk}}e^{(-1)^k i\alpha}$$

$$
\begin{aligned}
&-\frac{i\Gamma}{2\pi}\{\log[z-(\zeta)_p]\\
&\quad+\Big[\sum_{j=1}^{2}\sum_{k=1}^{M_j}(-1)^k\log(z-\zeta_{jk})\Big]\\
&\quad+\log[z-\zeta_{(3-p)(M_j+1)}]\}
\end{aligned}
\tag{6.1}
$$

where p ; 1 or 2 according to the cylinder from which the vortex is shed.

The last term in the curly bracket is required because the image vortices appear as a pair at all the stages or, in other words, to make the total circulation vanish.

7. Calculated examples

Streamlines obtained from the present investigation are shown in the Appendix for a number of different flow situations. In each situation, the plotted region is covered by a grid system and the value of the complex potential is calculated at every nodal point. Then the streamlines are generated by tracing the contours of constant value of the stream function.

The employed mesh size is typically 0.02 in both x- and y-direction but with more dense nodes at the adjacent region of the cylinders. The series were truncated using 0.0001 as the truncation parameter for both ε_μ and ε_ν.

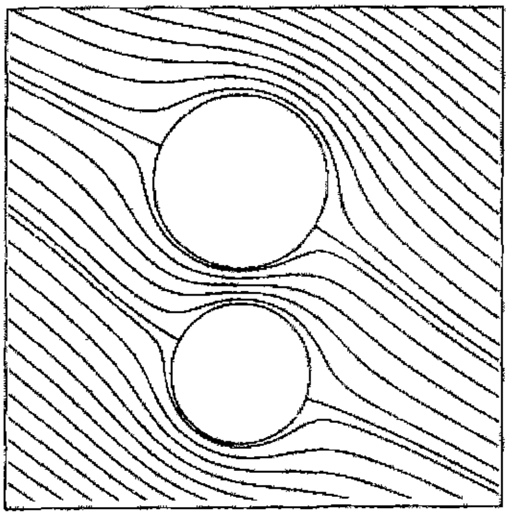

r=0.8 s=2.2 α=−30°

Figure. 3 Uniform flow

Figure 3 shows the streamlines of a uniform stream approaching the cylinders with the angle α=-30° . Figure 4 shows the streamlines when there is a single vortex, supposedly shed from the major cylinder, at the position (1.2, 1.6) with the center of the major cylinder at (0,1.2). In this case, the stream function was nondimensionalized with respect to the vortex strength. The other parameters are shown in the figure. Figure 5 shows the case of two cylinders introduced in the flow field that has been created by a vortex. This is the situation stipulated by the Milne-Thomson's circle theorem. The computational parameters have the same values as those of Figure 4. The difference between these two cases is that the total vortex strength in the flow field of the former case is nil whereas that of the latter is the strength of the vortex. When a uniform flow with the approaching angle α=30° is superposed to the situation of Figure 4, we have the streamline distribution shown in Figure 6. Only the nondimensional vortex strength is an additional parameter and has been set to 5.0. This case constitutes the basic building block in applying the present method to the vortex shedding simulation with multiple discrete vortices.

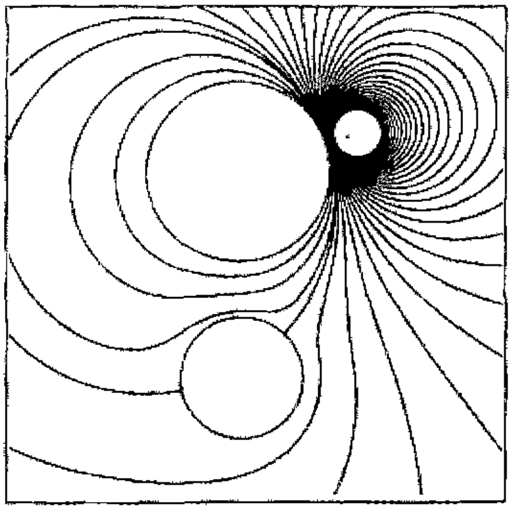

r=0.7 s=2.4 ζ=(1.2, 1.6)

Figure. 4 Two cylinders with a single vortex

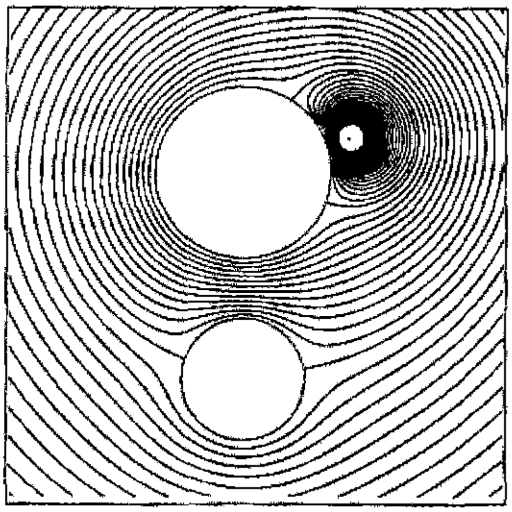

r=0.7 s=2.4 ζ=(1.2, 1.6)

Figure. 5 Flow by a vortex

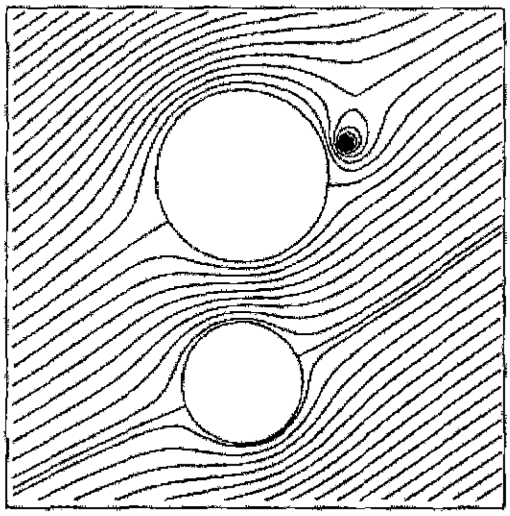

r=0.7 s=2.4 ζ=(1.2, 1.6)

Figure. 6 Uniform flow and a single vortex

8. Conclusions

The presented streamlines seem to provide sufficient ground to believe that the suggested way of tackling the problem is truly reliable.

Treatment of the series in connection with determining the truncation position might have at first sight appeared rather rough. If it were concerned with converging property of the series themselves, rigor is of course a crucial factor to be respected. But to find the truncation position only, it seems to be justifiable that the present treatment be adequate enough. In fact, the comment may be added that an appreciable margin can be expected if the suggested way of truncation is employed to acquire the accuracy in mind.

The same principle of building up the image singularity system can be extended to the situation of more than two circular cylinders placed in any arbitrary fashion. From practical point of view, only the complexity grows almost prohibitively with increase of the number of cylinders. However, if the image singularity system is sought through analytical means there can be no alternative other than the present way of approaching the problem.

References

Abramowitz, M and Stegun, I.A., Handbook of Mathematical Functions, Dover, 1972

Currie, I.G., Fundamental Mechanics of Fluids, McGraw-Hill, 1974

Milne-Thomson, L.M., Theoretical Hydrodynamics, 5th ed., Macmillan, 1968